



Environment
Canada

Environnement
Canada

National Hydrology Research Institute

NHRI PAPER NO. 3

IWD TECHNICAL BULLETIN NO. 110

Frost Gauges and Freezing Gauges

J.A. Banner and R.O. van Everdingen

NHRI

NATIONAL HYDROLOGY RESEARCH INSTITUTE,
INLAND WATERS DIRECTORATE,
OTTAWA, CANADA, 1979.



Environment
Canada

Environnement
Canada

National Hydrology Research Institute

NHRI PAPER NO. 3

IWD TECHNICAL BULLETIN NO. 110

Frost Gauges and Freezing Gauges

J.A. Banner and R.O. van Everdingen

NHRI

NATIONAL HYDROLOGY RESEARCH INSTITUTE,
INLAND WATERS DIRECTORATE,
OTTAWA, CANADA, 1979.

© Minister of Supply and Services Canada 1979

Cat. No. En 36-503/110

ISBN 0-662-10535-4

Contents

	Page
ABSTRACT	v
RÉSUMÉ	v
INTRODUCTION	1
APPARATUS	2
Electrical frost and freezing gauges	2
Visual frost gauges	5
INSTALLATION PROCEDURE	5
MEASUREMENTS AND DATA CONVERSION	6
RESULTS	7
COMPARISON OF RESULTS FROM DIFFERENT GAUGE TYPES	15
RELIABILITY	16
Changes in contact resistance with time	16
Cumulative changes in resistance, type III gauges	16
Leakage and potential damage from freezing, type III gauge	17
CONCLUSIONS	17
REFERENCES	17

Table

1. Depth of electrodes for freezing gauges at the 16th Avenue seepage site (a) type I gauge (b) type II gauge	7
--	---

Illustrations

Figure 1A. Resistivity for several soils and one rock type as a function of temperature	1
Figure 1B. Resistance of saturated sandy silt (16th Avenue seepage site, Calgary) as a function of temperature	2
Figure 2A. Construction details of type I freezing gauge	2
Figure 2B. Construction details of type II freezing gauge	3
Figure 2C. Construction details of type III frost gauge	3
Figure 2D. Construction details of type IV gauge	4

Illustrations (Cont.)

Figure 3.	High-resistance zone resulting from inadequate backfill (type I freezing gauge) . . .	5
Figure 4.	Comparison of results for two measurement methods: (1) single-electrode method and (2) electrode-pair method	6
Figure 5A.	Resistance vs. time for the type I freezing gauge at the 16th Avenue seepage site, 1973-74	8
Figure 5B.	Resistance vs. time for the type II freezing gauge at the 16th Avenue seepage site, 1973-74	9
Figure 5C.	Depth of freezing vs. time for the type I freezing gauge at the 16th Avenue seepage site, 1973-74	10
Figure 6.	Resistance (in $k\Omega$) as a function of depth and time, for the type I freezing gauge in saturated sandy silt at the 16th Avenue seepage site, 1973-74	11
Figure 7.	Resistance (in $k\Omega$) as a function of depth and time for the <i>outer</i> portion of the type IV combination gauge at the experiment site, 1974-75	11
Figure 8.	Resistance (in $k\Omega$) as a function of depth and time for the type I freezing gauge at the experiment site, 1974-75	12
Figure 9.	Resistance (in $k\Omega$) as a function of depth and time for the <i>inner</i> portion of the type IV combination gauge at the experiment site, 1974-75	12
Figure 10.	Temperature (in $^{\circ}\text{C}$) as a function of depth and time for the type I gauge at the experiment site, 1974-75	13
Figure 11.	"Slope" of resistance vs. time for individual electrodes of the type IV freezing gauge at the experiment site, 1974-75	14
Figure 12.	Resistance (in $k\Omega$) as a function of depth and time for the type III frost gauge at the experiment site, 1974-75	14
Figure 13.	"Possible freezing" period and depth indicated by the thermistors in the type I freezing gauge, by resistance measured in the type IV frost gauge, and by the visual frost gauges V_1 and V_2 at the experiment site, 1974-75	15
Figure 14.	Cumulative changes in resistance in the type III frost gauge at the experiment site, 1975-76	16

Abstract

Several types of frost gauges to detect frost (temperatures at or below 0°C) and several types of freezing gauges to determine the occurrence and extent of soil freezing (conversion of soil moisture from liquid to solid) were designed and constructed. The multisensor electrical-resistance freezing gauges enable determination of the progress, with time, of freezing and thawing in both saturated and unsaturated soils. In the case of unsaturated materials, the use of temperature sensors or electrical-resistance or visual frost gauges makes it possible to distinguish between the resistance effects of freezing and those of drying of the soil. Computer-generated plots of resistance vs. depth and time are used in the interpretation of the data. Best results are obtained when freezing gauges with small electrode spacings, installed directly in the soil, are measured daily.

Résumé

On a conçu et construit plusieurs genres de détecteurs de gel pour la détection du gel (températures égales ou inférieures à 0°C) et plusieurs genres de détecteurs de congélation permettant de déterminer l'existence et l'importance de la congélation du sol (passage de l'état liquide à l'état solide de l'humidité du sol). Les détecteurs de congélation à capteurs multiples qui mesurent des variations de résistance électrique permettent de déterminer l'évolution, en fonction du temps, de la congélation et de la décongélation des sols saturés et des sols insaturés. Pour les matériaux insaturés, l'utilisation de capteurs thermiques, de détecteurs de résistance électrique ou de détecteurs visuels permet de distinguer les conséquences de la congélation de celles de l'assèchement du sol sur la résistance. Des graphiques de la résistance en fonction du temps et de la profondeur, produits par ordinateur, sont utilisés pour l'interprétation des données. Les meilleurs résultats sont obtenus de détecteurs de congélation dont les électrodes sont faiblement espacés, installés directement dans le sol et dont on effectue quotidiennement la lecture.

Frost Gauges and Freezing Gauges

J.A. Banner and R.O. van Everdingen

INTRODUCTION

A simple and accurate method for determining the rate and depth of freezing and thawing in soil materials is required for both monitoring and research purposes in areas of seasonal and perennial frost.

Frost tubes (containing water and an indicator dye) for visual determination of the depth of the 0°C isotherm in freezing and thawing soils have been described by Rickard and Brown (1972) and Mackay (1973). Automated or remote readings are impossible with these devices. Also, the access tubes for the frost tubes have to protrude above the maximum expected snow level; access for daily readings will lead to packing of the snow, and elevated boardwalks to avoid snow packing will affect insolation. All of these, as well as the daily extraction of the frost tubes for readings, will affect the thermal regime in the soil to some extent.

A further, and perhaps more important, disadvantage is that freezing of the soil material around the frost tube may be considerably delayed (as compared to the freezing of the liquid inside the frost tube) by depression of the initial freezing point in the soil/water/solutes system. A similar disadvantage exists when thermocouples, thermistors or diodes are used in studies of soil freezing, because a temperature just below 0°C does not necessarily mean that the ground is frozen (i.e. containing at least some ice).

Both liquid and frozen water contents have a significant influence on the mechanical behaviour as well as on the electrical characteristics of a soil material (e.g. Anderson and Morgenstern, 1973). The changes in electrical resistivity of soil materials in response to freezing and thawing have been well documented in the literature (Garstka, 1944; Colman and Hendrix, 1949; Sartz, 1967; see Fig. 1A). The rapid increase in electrical resistance of a soil/water system upon freezing (Fig. 1B) and the corresponding decrease upon thawing provide a better method for detection of actual freezing (ice formation) than either temperature measurements or visual frost tube observations (Sartz, 1967).

Some success was obtained by Harlan *et al.* (1971) using individually installed Colman fibreglass soil moisture cells as indicators of freezing and thawing. Further experiments with multisensor electrical-resistance frost and freezing gauges were initiated by the Hydrology Research Division in the fall of 1972. Various modes of construction were tried to test (1) ease of construction and relative cost; (2) performance and (3) reliability.

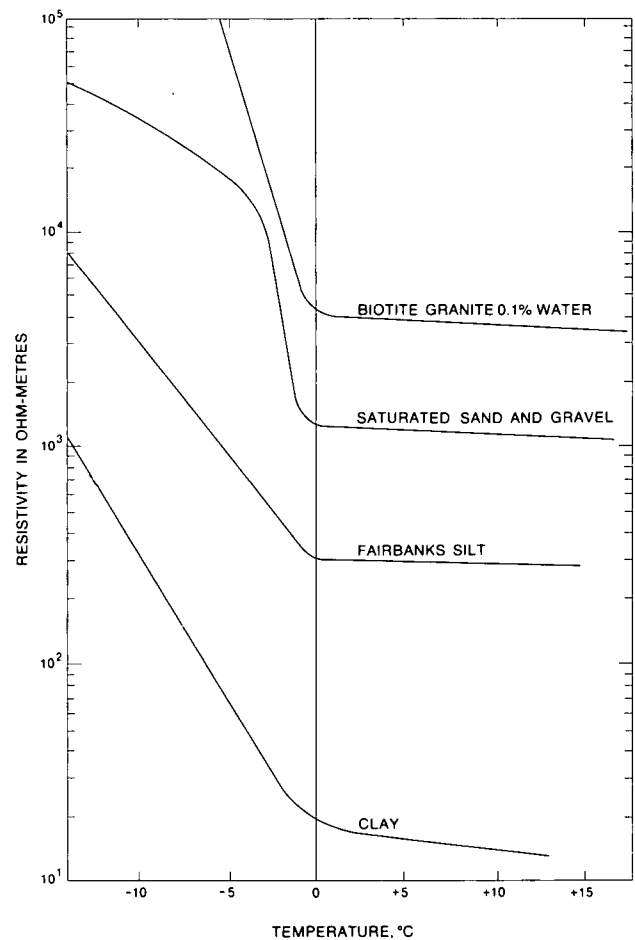


Figure 1A. Resistivity for several soils and one rock type as a function of temperature (Hoekstra and McNeill, 1973).

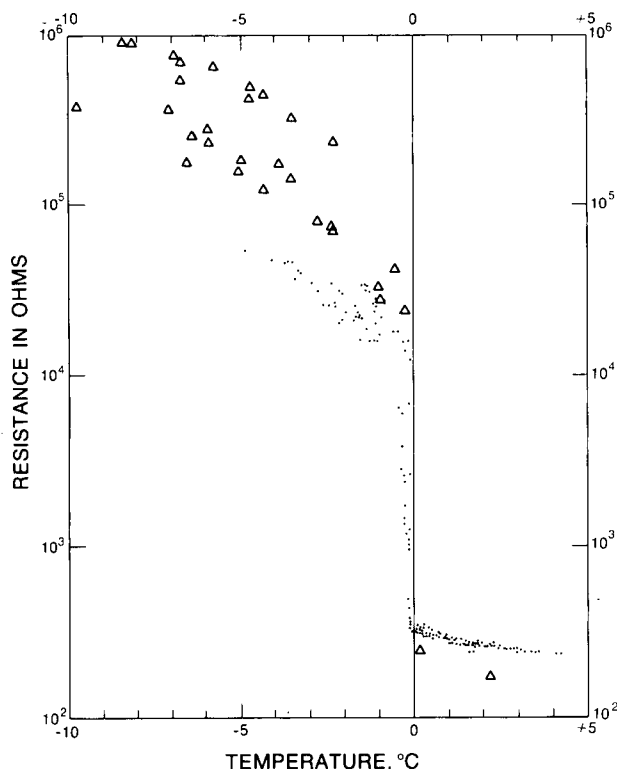


Figure 1B. Resistance of saturated sandy silt (16th Avenue seepage site, Calgary) as a function of temperature. Triangles represent values for upper electrode in contact with material subject to drying.

Frost tubes of the type described by Rickard and Brown (1972) were used for comparison purposes. Various modifications of such visual frost gauges were tested in an attempt to improve their performance.

This report describes the results of the experiments with both electrical and visual gauges.

APPARATUS

Electrical Frost and Freezing Gauges

The electrical-resistance frost and freezing gauges consisted of two or more metal electrodes, spaced at regular or irregular intervals. The electrodes were either mounted on an insulating carrier or separated by insulators. The frost-gauge electrodes were placed in contact with a self-contained filling of water to detect frost (occurrence of temperatures at or below 0°C), while the freezing-gauge electrodes were placed so as to contact the surrounding soil to detect freezing. Electrode spacings (centre to centre) ranged from 50 to 165 mm (gaps between electrodes from 10 to 128 mm); surface areas of individual electrodes were 3, 6, 14 or 35 cm². The gauges were installed in the

ground in augered or drilled holes; ground elevations and the elevations of the gauges were determined shortly after installation. Wiring from groups of frost and/or freezing gauges was run to convenient measuring locations.

Four different modes of construction, designated types I to IV, were developed and tested. General construction and installation details are given below (see Figs. 2A-D).

The first *type I freezing gauge* was constructed in November 1972. It consisted of stainless steel electrodes

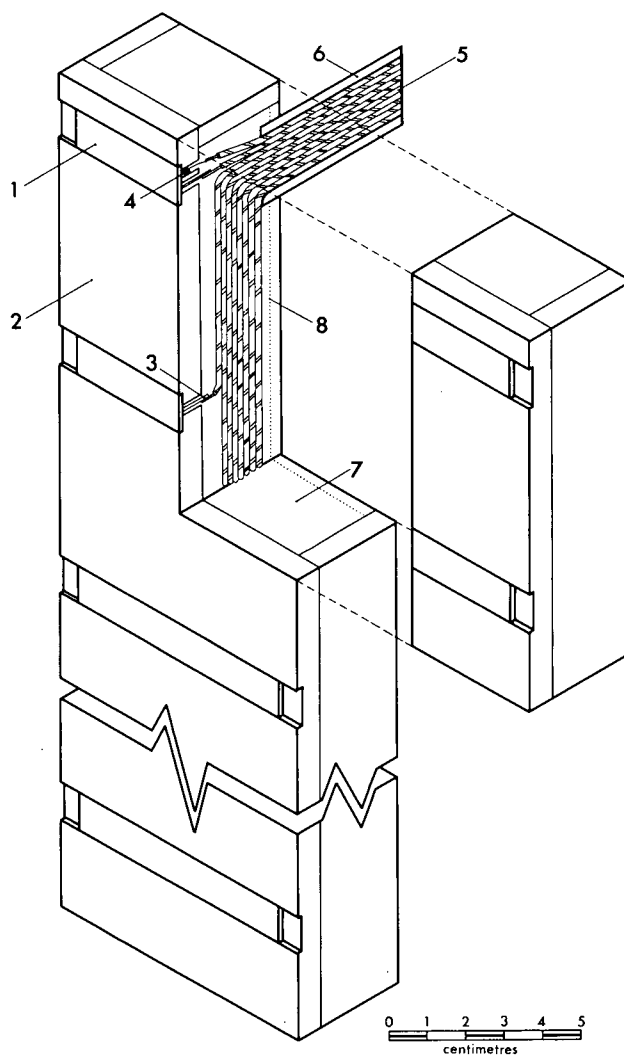


Figure 2A. Construction details of type I freezing gauge. Stainless steel plates (1) were epoxied into shallow recesses in the front of a sheet-acrylic trough (2), after stubs (3) were brazed on. Stubs and thermistors (4) were soldered to connecting wires (5), which entered the gauge via 21.3-mm (1/2 in. pipe size) PVC conduit (6). The trough was then filled with casting acrylic (7), which embedded the wiring, and a layer of reinforcing fibreglass (8).

set at precisely equal intervals in an acrylic bar (Fig. 2A). YSI type 44004 thermistors were mounted behind and in contact with some of the electrodes to measure temperature.

This gauge was installed in a 23-cm (9-in.) augered hole in silt, at the experiment site behind the building of the Institute of Sedimentary and Petroleum Geology (ISPG) in Calgary on November 8, 1972.

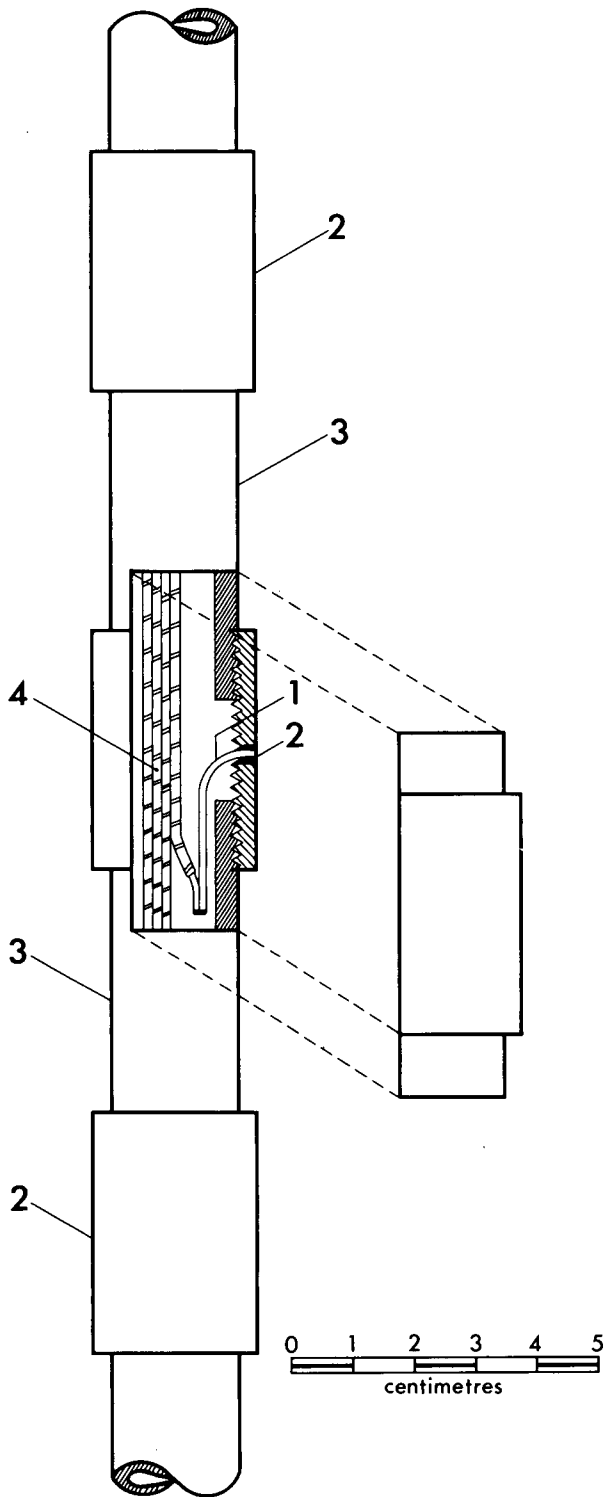


Figure 2B. Construction details of type II freezing gauge. Wire stubs (1) were soldered into holes drilled in 21.3-mm (1/2 in. pipe size) galvanized steel pipe couplings (2). Couplings were spaced with 21.3-mm (1/2-in. pipe size) threaded PVC nipples (3) of various lengths. A connecting wire (4) was soldered onto each stub before the next lower nipple was screwed into the coupling. Joints were made watertight with Teflon tape.

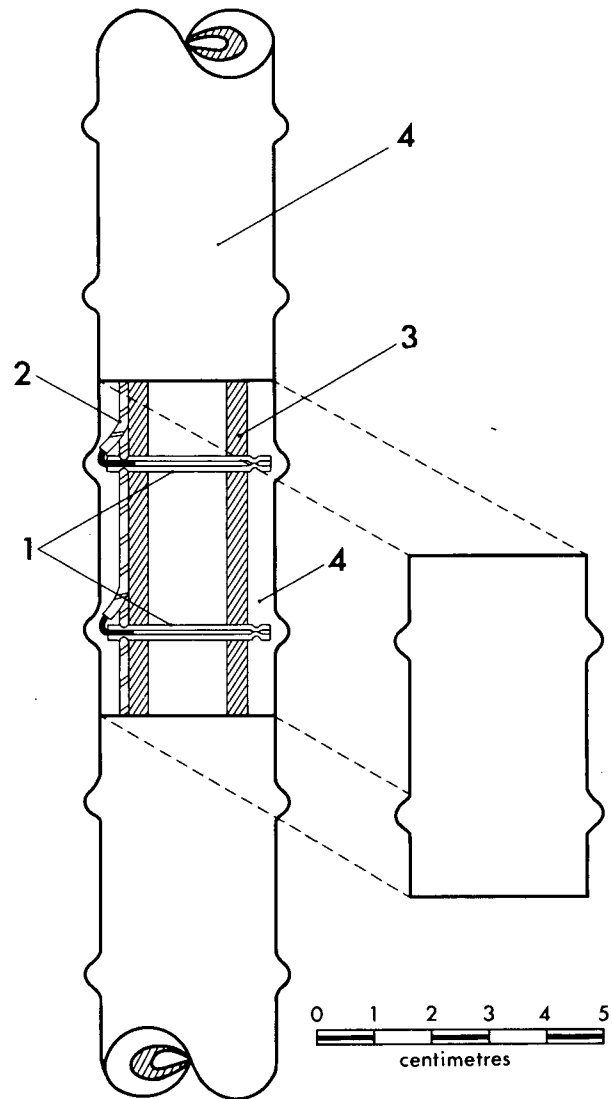


Figure 2C. Construction details of type III frost gauge. 3.2-mm (1/8 in.) stainless steel tubes (1) with connecting wires (2) crimped into one end were inserted into holes drilled at 3-cm intervals in a length of 21.3-mm (1/2-in. pipe size) PVC pipe (3); the other ends of the small tubes were then crimped to retain the tubes in place. The gauge was waterproofed with two wraps of self-vulcanizing rubber tape, followed by two wraps of plastic tape (4). The bottom end was closed with a 21.3-mm (1/2-in. pipe size) PVC cap (not shown), the pipe was filled with 3-mm styrofoam balls and water, and the top plugged with a small cork (not shown).

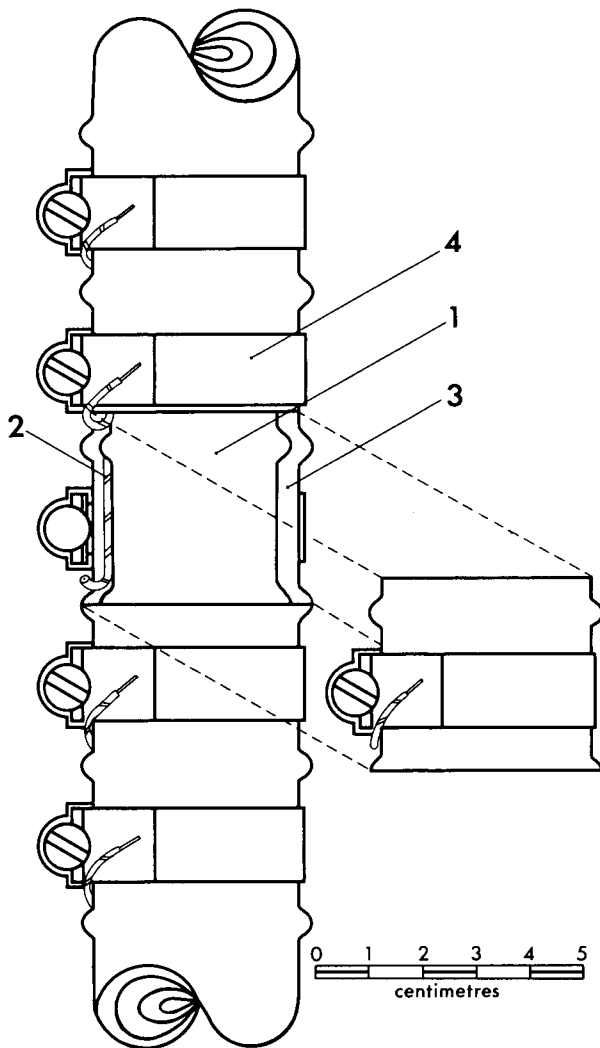


Figure 2D. Construction details of type IV gauge. A type III gauge (1), lacking only the outer two wraps of plastic tape and equipped with a second set of connecting wires (2), was wrapped with two layers of self-vulcanizing rubber tape (3), through which the connecting wires were allowed to protrude at 3-cm intervals. Tridon type HS-16 stainless steel hose clamps (4) were secured around the gauge at intervals of 3 cm; one of the protruding connecting wires was soldered to each clamp.

A similar type I freezing gauge was operated from November 2, 1973, to May 16, 1974, at a groundwater seepage site in sandy silt along 16th Avenue in northeast Calgary. It was then moved to the Norman Wells test section of the Hydrology Research Division where it was operated from June 1974 to September 1975 (van Everdingen and Banner, 1975).

Type II freezing gauges were first constructed in November 1973. They were made of 21.3-mm (½-in. pipe size) galvanized pipe couplings serving as electrodes, which were separated by plastic pipe nipples of various lengths as insulators (Fig. 2B).

A short (38.5 cm) type II freezing gauge was operated from November 2, 1973, to May 16, 1974, at the groundwater seepage site in northeast Calgary. Three more, varying in length from 4.25 m to 4.93 m, were installed in 13-cm-(5-in.-) dia. drillholes in silt at the Frost Effects Test Facility of Canadian Arctic Gas Study Limited (CAGSL) in northwest Calgary, on February 26, 1974, to monitor development of the frozen-ground envelope adjacent to chilled-air pipeline test sections. One of these gauges was destroyed by construction equipment in September 1977.

To help distinguish between high resistance caused by drying of the soil and that caused by freezing, the type I freezing gauge employed thermistors. A similar purpose is served by the closed-system *frost gauge, type III*. It was constructed from 21.3-mm (½-in. pipe size) PVC pipe, using short pieces of 3.18-mm (¼-in.) stainless steel tubing placed radially through the plastic pipe as electrodes (Fig. 2C). The internal filling initially consisted of small styrofoam balls (to accommodate expansion upon freezing) and tap water.

One type III frost gauge was installed at the experiment site behind the ISPG in Calgary on September 18, 1974. It was placed in a 48.3-mm (1½-in. pipe size) ABS access pipe installed in an 8-cm-(3-in.) dia. augered hole, which was backfilled with slurried original soil material. During the summer of 1975 it became apparent that this frost gauge was not performing satisfactorily (see under Results). The styrofoam was removed and the tube refilled with tap water on October 2, 1975. On September 30, 1977, the gauge was removed and dismantled to check on leakage and possible failure of the plastic pipe which might have resulted from freezing.

The *type IV gauge* was constructed to combine the frost-detecting capability of the type III frost gauge with freezing detection through the use of stainless steel hose clamps fastened as electrodes around the outside of a type III gauge (Fig. 2D).

This combination frost-and-freezing gauge was installed in an 8-cm (3-in) augered hole at the experiment site behind the ISPG; the hole was backfilled with slurried original soil material. Because of unsatisfactory performance of the internal frost-detection portion of this gauge (see under Results), the styrofoam filling was removed and the tube refilled with tap water on October 2, 1975.

An additional type of frost gauge, consisting of an electrode pair in a small sealed water-filled compartment, was constructed in prototype and tested in a coldroom; it has not been field-tested. It is mentioned here, however, because it appears to offer a possible solution to the problems encountered with the type III frost gauge.

Visual Frost Gauges

For comparison, visual frost gauges of the type described by Rickard and Brown (1972) were used in 26.7-mm ($\frac{3}{4}$ -in. pipe size) PVC access tubes that were installed in augered holes at the experiment site at the ISPG building in Calgary on September 18, 1974. The first two frost gauges were made of 12.7-mm ($\frac{1}{2}$ -in.) O.D. nylon tubing, one (V1) filled with 3-mm styrofoam balls (to absorb freezing expansion), the other (V2) filled with 200- μ m glass beads. Both were then saturated with a 0.1% solution of sodium fluorescein in water. The exact level to which the fluorescein solution had changed colour upon freezing proved to be difficult to detect in both

gauges. Consequently, both gauges were replaced on October 15, 1975. One replacement consisted of a nylon tube containing a 0.1% sodium fluorescein solution and white sand; the other consisted of a clear acrylic tube containing a solution of 0.01% bromthymol blue (indicator dye) and 0.1% NaHCO_3 (for pH stabilization) and styrofoam balls. The blue colour of bromthymol indicator solution vanishes upon freezing. Both visual frost gauges were removed on September 30, 1977.

INSTALLATION PROCEDURE

With one exception, all the frost and freezing gauges were installed in 8-cm (3-in.) or 13-cm (5-in.) holes drilled

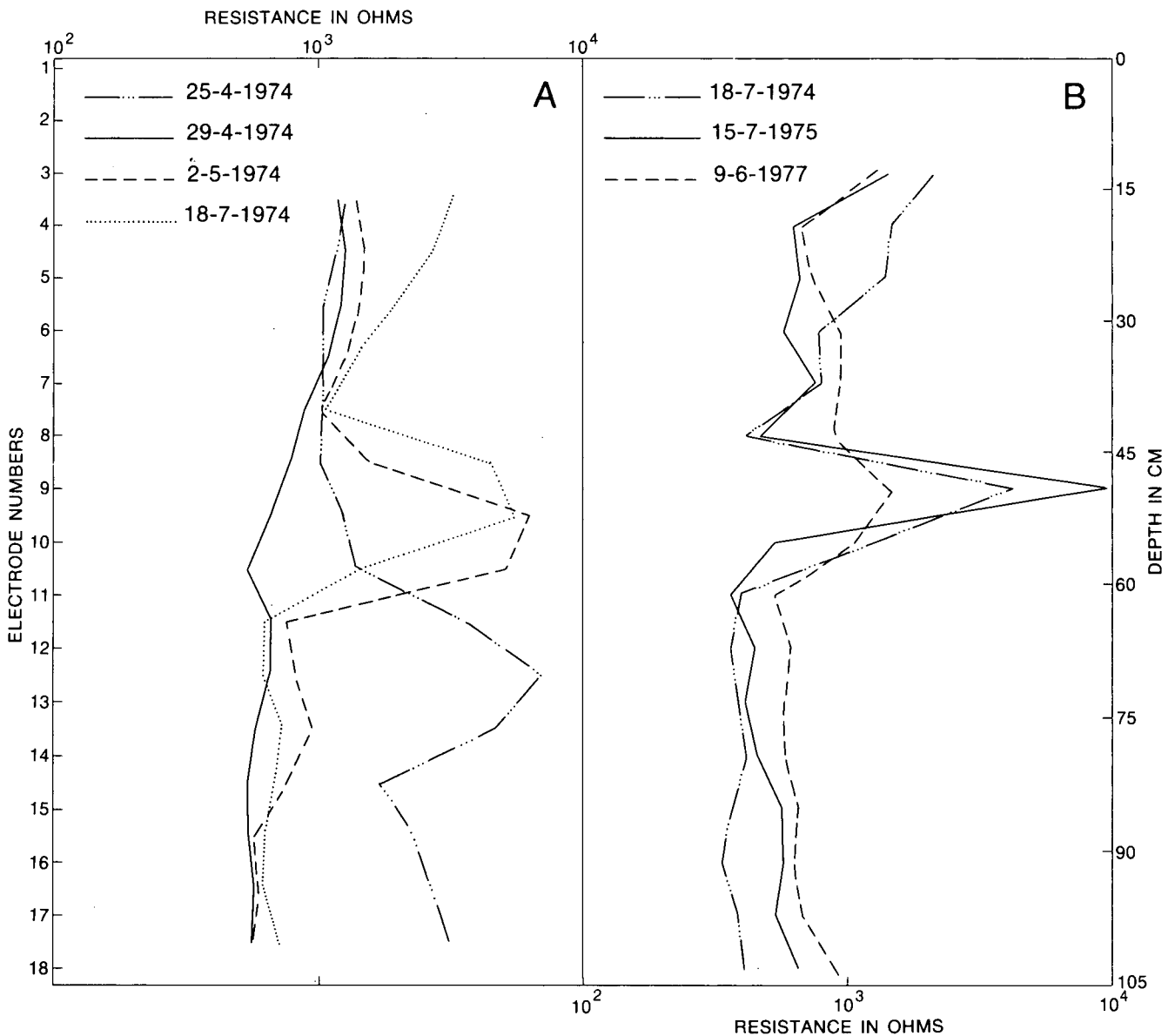


Figure 3. High-resistance zone resulting from inadequate backfill (type I freezing gauge). (A) Upward displacement of high-resistance zone during strong recharge event (snowmelt plus rain) during late April, 1974 (measured by the electrode-pair method). (B) Position of high-resistance zone has been stable since July 18, 1974 (measured by the single-electrode method).

with a power auger. The first freezing gauge at the experiment site was installed in a 23-cm (9-in.) augered hole to facilitate rapid backfilling and tamping. This procedure, however, turned out to have shortcomings: it is time consuming and the results are not always satisfactory. Figure 3a shows a high-resistance "zone" centred around electrodes 12 and 13 of the type I freezing gauge (April 25, 1974). A very strong recharge event, recorded in the week of April 29, 1974, resulted in a two-stage upward displacement of the high-resistance zone (resistance plots for May 2 and July 18, 1974); the high-resistance zone has been stationary since that time (Fig. 3b, resistance measured by the single-electrode method). This sequence of events has been interpreted as reflecting poor contacts resulting from inadequate backfill; the strong recharge event of late April 1974 caused downward redistribution of material in the backfill, resulting in the upward displacement of the zone with poor contact.

To avoid this problem, all other frost and freezing gauges were installed with a slurried or very carefully tamped backfill.

MEASUREMENTS AND DATA CONVERSION

A special 72-Hz Wheatstone bridge with phase-sensitive detector and automatic gain control was developed to enable measurement of resistance between electrodes without interference from power lines or polarization problems. The indicator meter of the instrument is balanced by adjusting a ten-turn potentiometer with a three-digit readout. After the meter is balanced, the reading is recorded.

The accuracy of the resistance measurements varies from about $\pm 5\%$ at 100 ohms to better than $\pm 0.6\%$ between 1000 and 90 000 ohms, rising again to about $\pm 5\%$ at 10^6 ohms. As frost gauges and freezing gauges are primarily intended to determine the position, in both space and time, of the strong resistance contrast between frozen and non-frozen material (Fig. 1), this accuracy is more than adequate.

The resistance measured is a function of resistivity, electrode configuration and measurement method. The resistivity, in turn, is a function of the mineralogy and grain size distribution of the soil material, its water and dissolved solids contents and temperature. For permanently installed resistance gauges the soil mineralogy and grain size distribution normally remain constant; resistivity increases with decreasing temperature. Drying of the soil (which eliminates liquid water) has the same effect on electrical resistivity as freezing of the soil.

Electrode configuration has little effect on the measured resistance, lowering it somewhat when electrode

distance is very small or when electrode area is large, and raising resistance somewhat when electrode distance is very large or when electrode area is small. The surface area of individual electrodes must of course be large enough to provide adequate contact with the medium to be measured.

The measurement method can affect the measured resistance values and also the shape of any resistance vs. depth and resistance vs. time plots of the data.

Resistance can be measured either between pairs of adjacent electrodes on a gauge (electrode-pair method) or from each individual electrode in turn to a common

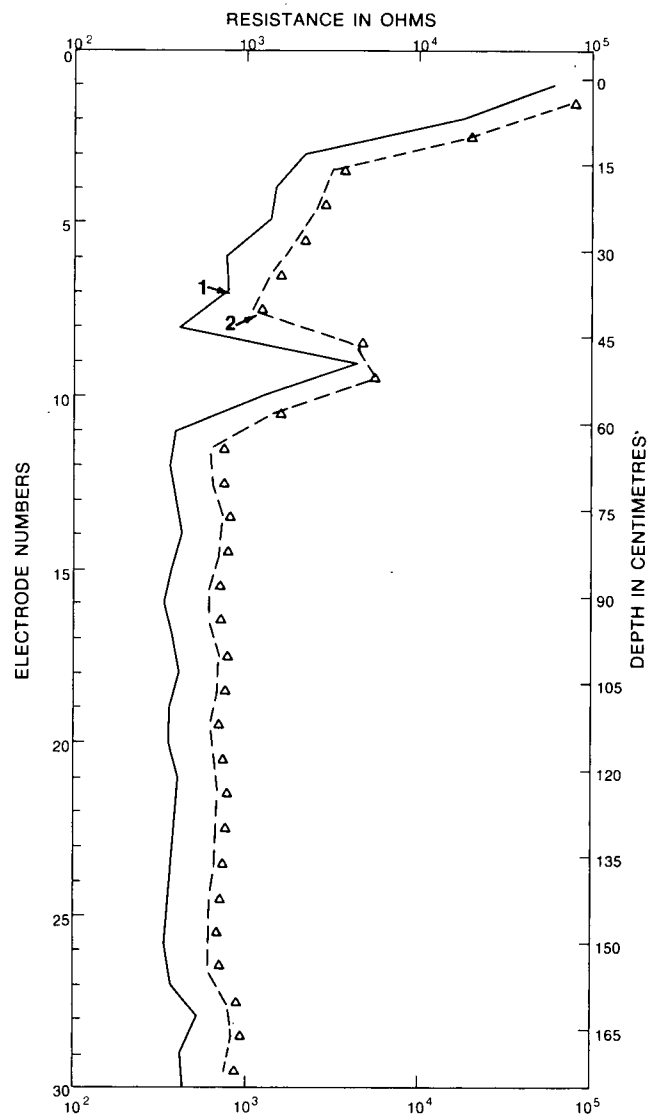


Figure 4. Comparison of results for (1) single-electrode method and (2) electrode-pair method. Also indicated (by triangles) are resistance values for pairs of electrodes, derived through addition of resistance values for individual electrodes measured by the single-electrode method.

“ground” consisting of all the other electrodes connected in parallel (single-electrode method). Figure 4 shows the differences in the resistance values obtained by the two methods applied to the same gauge on the same date. It should be noted that the measured values are plotted in the centre of each depth interval between adjacent electrodes for the electrode-pair method, and at the level of the centres of the individual electrodes for the single-electrode method.

The differences in shape between the two graphs in Figure 4 are also a direct result of the measurement method. This can be explained by considering an electrode in contact with high-resistivity material, juxtaposed with electrodes in contact with low-resistivity material; the result is two high resistance values when the electrode-pair method is used, but only one high resistance value, flanked by two low resistance values, when the single-electrode method is used.

Readings of the type II freezing gauges at the CAGSL Frost Effects Test Facility were taken using the electrode-pair method. The type I freezing gauge at the ISPG experiment site was read using both methods, whereas the type III frost gauge and the type IV combination gauge were read only by the single-electrode method. Whenever possible, readings were taken weekly; daily readings were obtained between November 20, 1974, and May 21, 1975.

A computer program, written in Fortran for the Univac 1108 at Computer Sciences Canada in Calgary, was used to convert the readings into resistance values. Output from the program is in the form of tables of resistance values for all electrodes (or electrode pairs) for each date of measurement. Plotting options allow a choice of three types of graph: resistance versus time for individual electrodes or electrode pairs (e.g. Fig. 5A); resistance versus depth for selected dates (e.g. Figs. 3 and 4); and resistance as a function of both depth and time (e.g. Fig. 6).

RESULTS

The simplest presentation of frost- or freezing-gauge results is a graph of resistance vs. time for each electrode or each electrode pair. Figures 5A and 5B show such graphs for a type I gauge and a type II gauge, respectively, both at the 16th Avenue site (measured by the electrode-pair method).

When the freezing front advances past the top of the *upper* electrode of an electrode pair, the measured resistance starts increasing; it usually increases by an order of magnitude or more by the time the freezing front advances past

the bottom of the upper electrode. After that the resistance may increase further or it may fluctuate, depending on the prevailing temperature conditions. During thawing from the surface downward, the resistance measured for an electrode pair will not start decreasing significantly until thawing reaches the *lower* electrode.

In Figure 5A the time intervals during which the soil adjacent to the upper electrode of successive electrode pairs froze are obvious from the periods of rapidly increasing resistance, which were preceded by relatively uniform low resistance values characteristic of the saturated conditions at the site and followed by relatively high resistance values which vary somewhat with the temperature of the soil. The rapid increases in resistance are analogous to the steep increases in resistivity shown in Figure 1A.

Table 1. Depth of Electrodes, in Millimetres below Ground, for Freezing Gauges at the 16th Avenue Seepage Site.

Electrode No.	Top	Base	Centre of Interval
TYPE I GAUGE			
1	4	14	39
2	64	74	99
3	124	134	159
4	184	194	219
5	244	254	279
6	304	314	339
7	364	374	399
8	424	434	459
9	484	494	519
10	544	T	579
11	604	614	639
12	664	674	699
13	724	734	759
14	784	794	819
15	844	T	879
16	904	914	939
17	964	974	999
18	1024	1034	1059
19	1084	1094	1119
20	1144	1154	1179
21	1204	1214	1239
22	1264	1274	1299
23	1324	1334	
TYPE II GAUGE			
1	24	79	103.5
2	128	165	171.7
3	178.5	204	211.2
4	218.3	244	250.5
5	257	282.5	288.2
6	294	332	337
7	342	382	386.5
8	391	432	

T – Thermistors.

Determination of the depth to which the ground was frozen at any particular time, however, requires reference to the depth of each of the electrodes (Table 1). Combining Figure 5A with Table 1 results in a plot of depth of freezing vs. time (Fig. 5C) which shows 'bars' that indicate the time period over which freezing (and later thawing) occurred in the depth interval adjacent to each electrode. Single 'bars' cover both the freezing and thawing period at the level of electrodes 11 and 12, because the soil adjacent to these electrodes did not freeze completely in the winter of 1973/1974. Lines connecting the corners of successive 'bars', as shown in Figure 5C, delineate the zone of *partially* frozen soil in both depth and time; the zone is divided into two portions, representing freezing from early November to late March and thawing from late March to mid-May. The

top of the partially frozen zone is poorly defined during March and early April.

The above two-step procedure can be simplified, and the poor definition of the partially frozen zone in late winter improved, by plotting contours of resistance against depth and time. Figure 6 shows this for the data from the type I gauge that were used in Figure 5C.

This computer-generated plot used logarithmic interpolation of resistance in both directions (depth and time axes) to plot continuous contours for selected values of resistance. For this interpolation process, the measured resistances were assigned to depths corresponding to the centres of the electrode-pair intervals when measured by

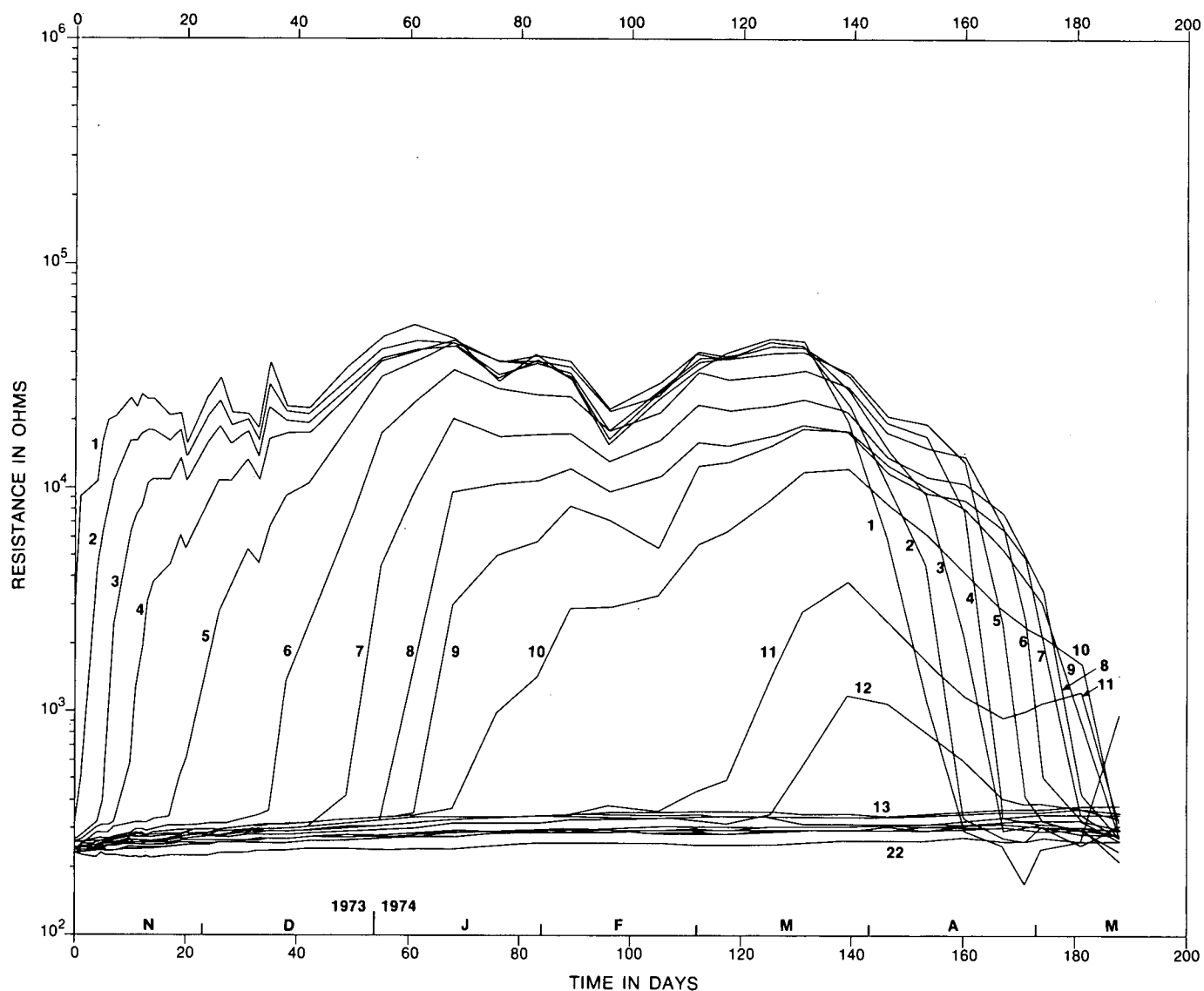


Figure 5A. Results obtained with gauge installed in saturated sandy silt at the 16th Avenue seepage site, 1973-74. Resistance vs. time for the type I freezing gauge (numbers are for electrode pairs).

the electrode-pair method, and to depths corresponding to the centres of individual electrodes when measured by the single-electrode method. This will tend to advance apparent freezing depth and apparent thawing depth by an amount not exceeding one half of the electrode spacing, when the electrode-pair measuring method is used.

Bunching of contours indicates when freezing or thawing occurs; it is analogous to the rapid rise of the resistance shown by the curves in Figure 5A. The doubt about the freezing in the interval between electrodes 10 and 12 is resolved; partial freezing can be seen to have occurred at these depths, because all contours up to 10 ($k\Omega$) crossed the depth of the 10th electrode, whereas only the 0.5 and 1.0 ($k\Omega$) contours crossed the depth of the 12th electrode.

Selection of different contour resistance values will influence the shape of the plot somewhat. If 1.0 $k\Omega$ had been selected as the lowest contour value, freezing would have appeared to start later at the same depth or to penetrate less deep at any particular time. It is important, therefore, that the contour values for such plots are selected carefully on the basis of observed resistances.

In unsaturated conditions, increases in resistance caused by drying of the soil tend to obscure increases in resistance caused by freezing. Figures 7 and 8 show contours of resistance vs. depth and time for freezing gauges of types IV and I, respectively, at the experiment site for the 1974-75 winter. Based on the position of the 0.5 $k\Omega$ contours, both figures appear to indicate freezing to a depth

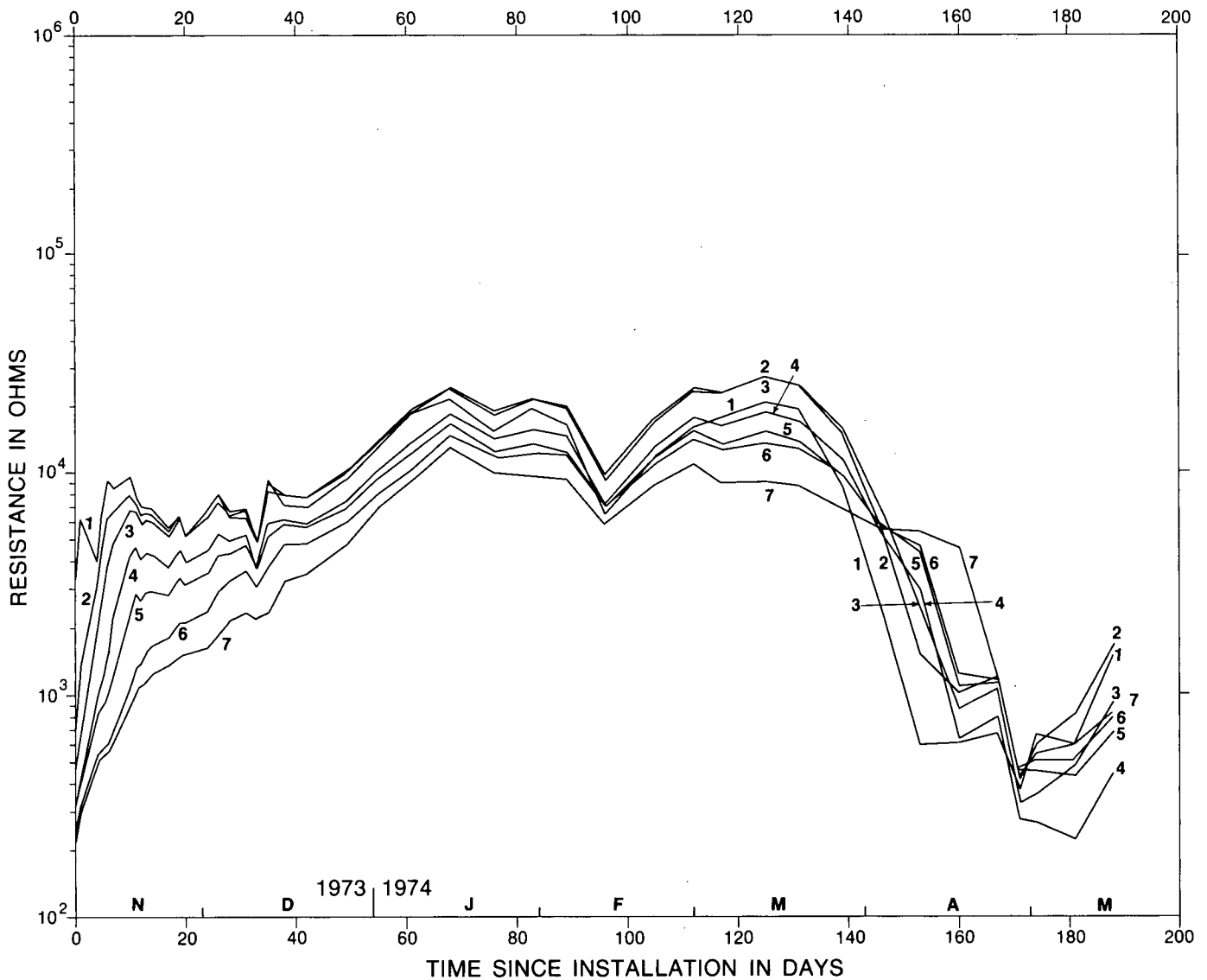


Figure 5B. Results obtained with gauge installed in saturated sandy silt at the 16th Avenue seepage site, 1973-74. Resistance vs. time for the type II freezing gauge (numbers are for electrode pairs).

of at least 40 cm by day 60. In fact, no freezing did occur until after day 60; the earlier crossing of a depth level by successive contours actually indicates increasing resistance because of drying. This can be confirmed by inspection of Figure 9, which shows contours of resistance vs. depth and time for the inner portion of the type IV gauge. The water-filled type III gauge, which forms the inner portion of the type IV gauge, operates in permanently saturated conditions (its own water filling) and exhibits resistance characteristics similar to those of type I and II gauges in saturated conditions; resistances have uniform, low values before freezing

and a sharp increase upon freezing, producing bunched contours as shown in Figure 9. Not until day 60 does the water in the inner portion of the type IV gauge begin to freeze, and only after this water starts to freeze can there be the possibility of the soil water (with its freezing point depressed by tension and dissolved solids) starting to freeze.

Similarly, for the type I freezing gauge, inspection of contours of temperature versus depth and time (Fig. 10) reveals that only after day 73 did the ground cool to 0°C,

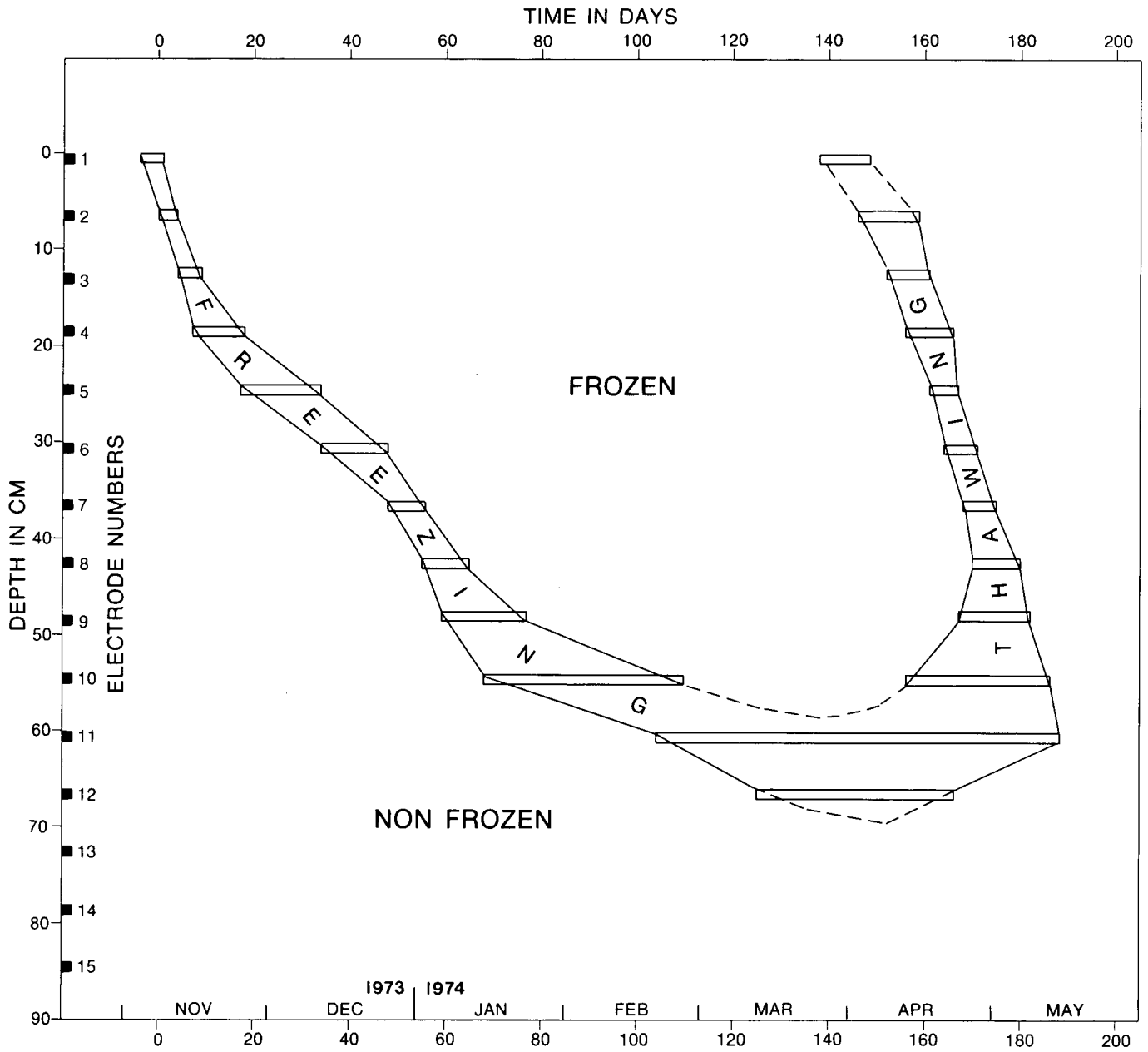


Figure 5C. Results obtained with gauge installed in saturated sandy silt at the 16th Avenue seepage site, 1973-74. Depth of freezing vs. time for the type I freezing gauge (numbers are for individual electrodes).

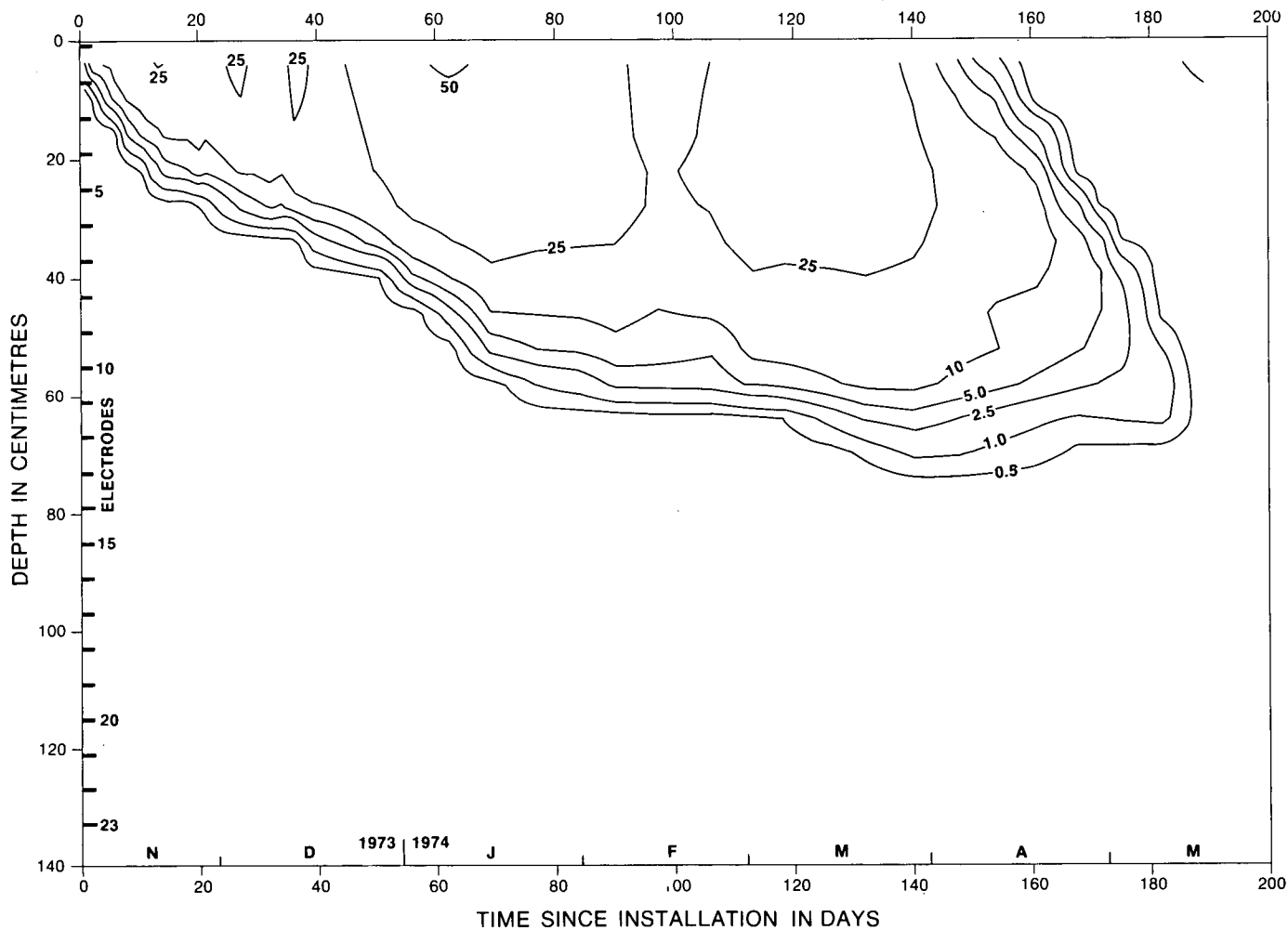


Figure 6. Resistance (in $k\Omega$) as a function of depth and time for the type I freezing gauge in saturated sandy silt at the 16th Avenue seepage site, 1973-74.

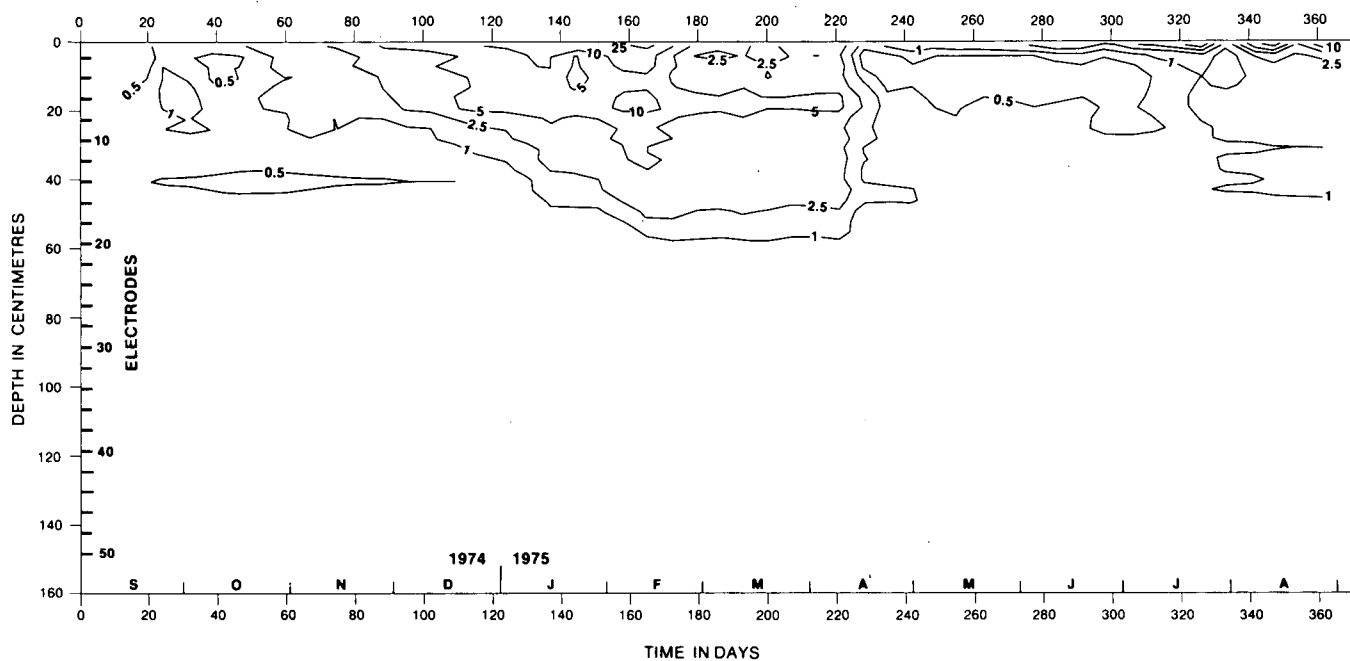


Figure 7. Resistance (in $k\Omega$) as a function of depth and time for the *outer* portion of the type IV combination gauge at the experiment site, 1974-75.

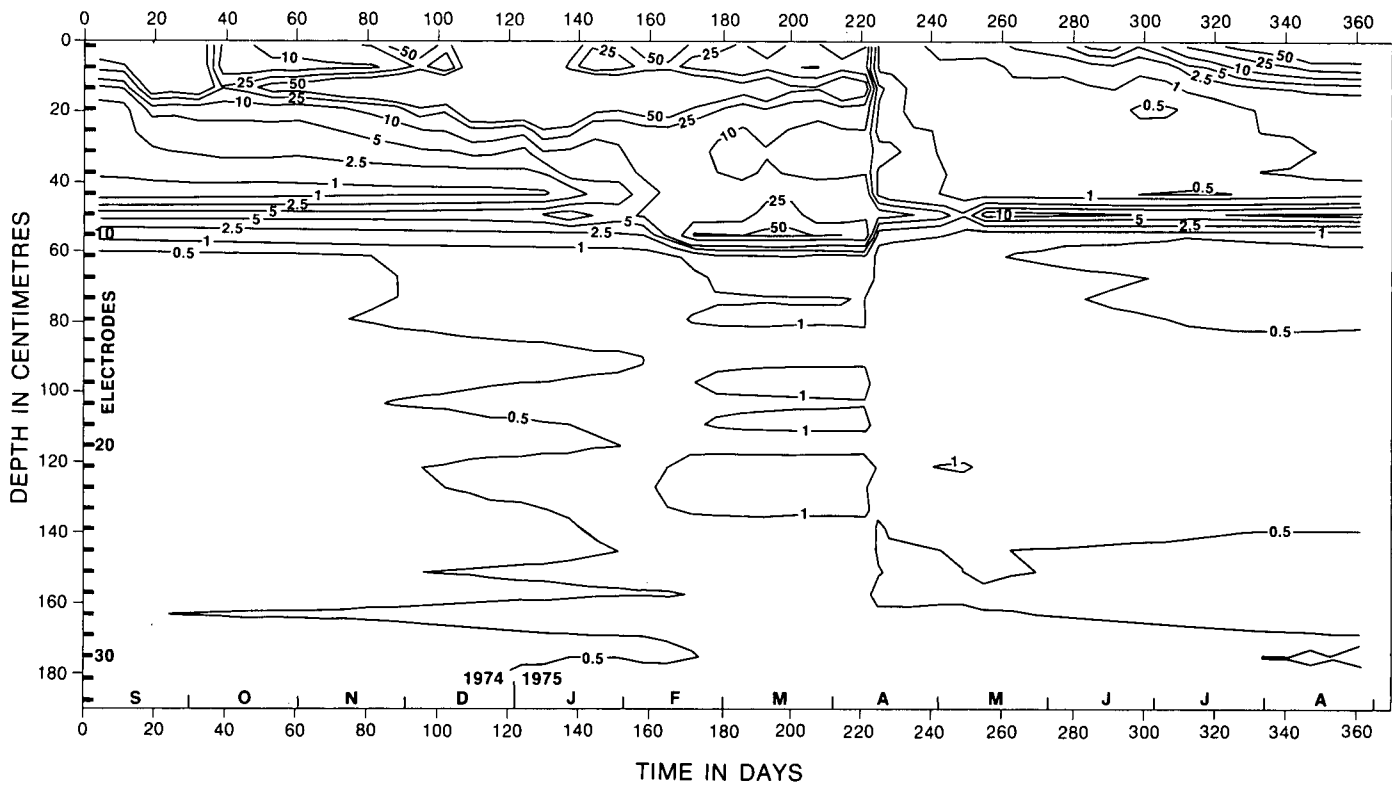


Figure 8. Resistance (in $k\Omega$) as a function of depth and time for the type I freezing gauge at the experiment site, 1974-75.

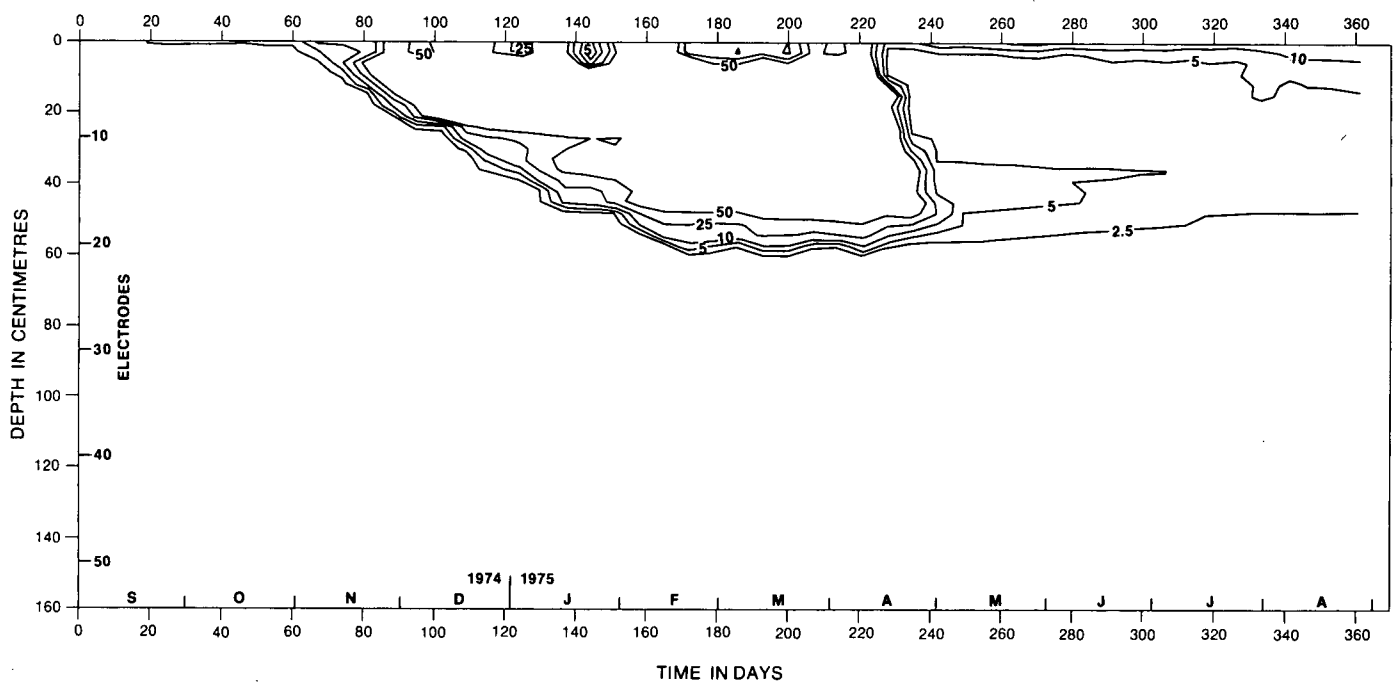


Figure 9. Resistance (in $k\Omega$) as a function of depth and time for the inner portion of the type IV combination gauge at the experiment site, 1974-75.

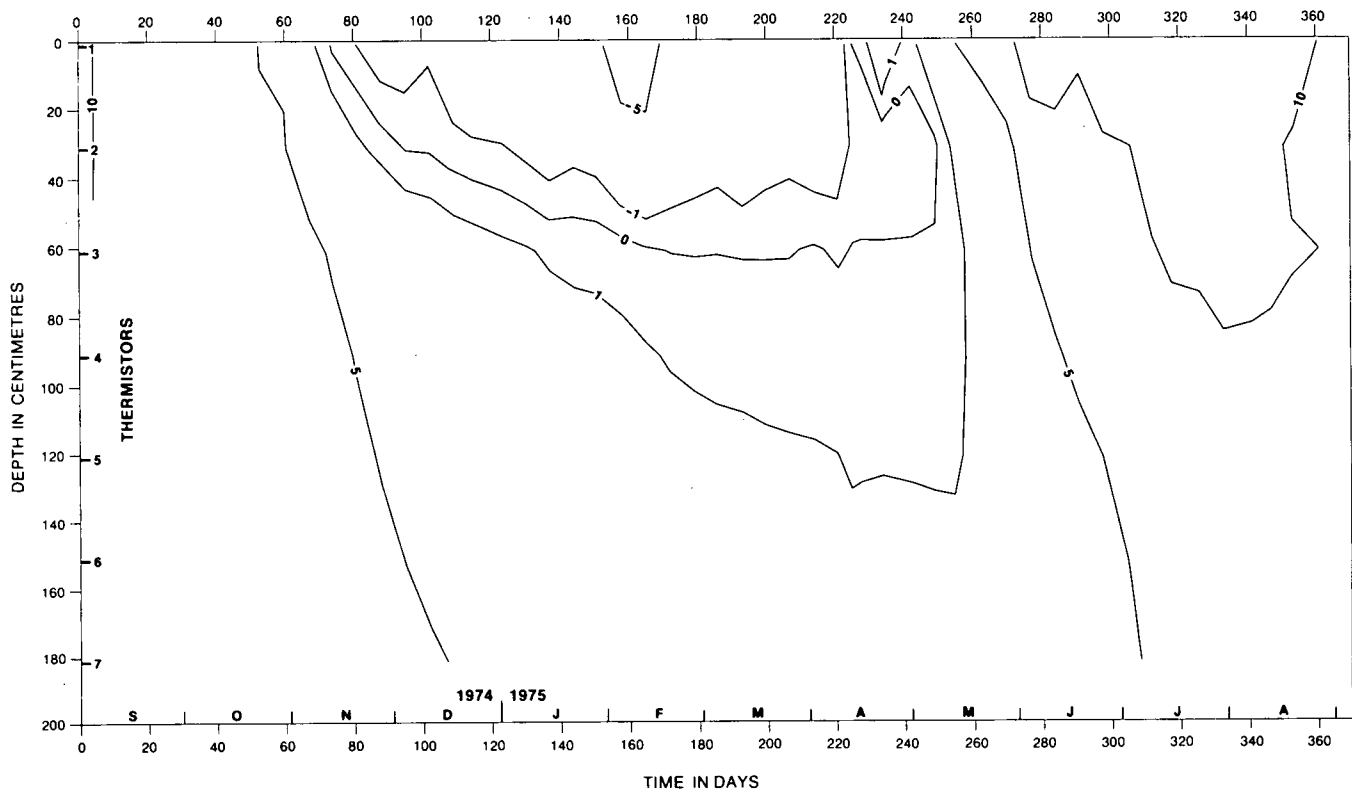


Figure 10. Temperature (in °C) as a function of depth and time for the type I gauge at the experiment site, 1974-75.

making it possible for freezing to begin. Referring to Figure 7 with this in mind, it can be seen that not until the period between days 78 and 85 did freezing advance past the first electrode.

The time/depth extent and degree of freezing can be followed through the freezing period by this method, keeping in mind that for the type I gauge, freezing can only occur within the boundaries of the 0°C isotherm (or "frost wedge", Harlan *et al.* 1971) and for the type IV gauge, within the "area of possible freezing" defined by the behaviour of its inner portion. It is also obvious that the bunched contours and high resistance at the level of the ninth electrode in Figure 8 cannot indicate a permanently frozen zone at a depth of 49 cm; rather, this is the result of the inadequate backfilling discussed earlier. Normally, data from such a known faulty electrode would be excluded from the plot.

Not immediately obvious from Figure 9 is that the possibility of freezing ended at day 250. The "tailing" of the 2.5 and 5 kΩ contours past this time seems to indicate that the inner portion of the type IV gauge was still partially frozen; this, however, was found to be the result of the slight salt content of the water filling having been flushed downward by freezing and not having had sufficient time to diffuse upward.

A second method to reduce the confusion between resistance increase due to freezing and resistance increase due to drying, and also to define more accurately the time/depth extent of freezing, makes use of the fact that the resistance increases relatively rapidly with freezing but only slowly with drying. This can be utilized by plotting the "slope" of the log of the resistance with respect to time. For this method to be fully effective, resistance should be measured daily. Results for the type IV gauge at the experiment site, for the period from 20 November, 1974, to 20 May, 1975, are shown in Figure 11, which is a plot of

$$f(R) = \pm \exp \left| \frac{\Delta \ln R}{D} \right|$$

where D is number of days between readings (normally 1); values of f(R) are positive for increasing R and negative for decreasing R. This is similar to slope, but it emphasizes the peaks somewhat. Values calculated for each electrode were plotted relative to a zero line representing the depth for that electrode. Values above the line indicate increasing resistance, those below it decreasing resistance. To simplify determination of "frozen" vs. "nonfrozen", the time intervals over which the inner electrodes of this gauge were frozen are shown. Also shown is a composite plot of mean daily air temperature measured near the site, at the University of Calgary, and at Calgary International Airport. Changes in the degree of freezing can be correlated with the air temper-

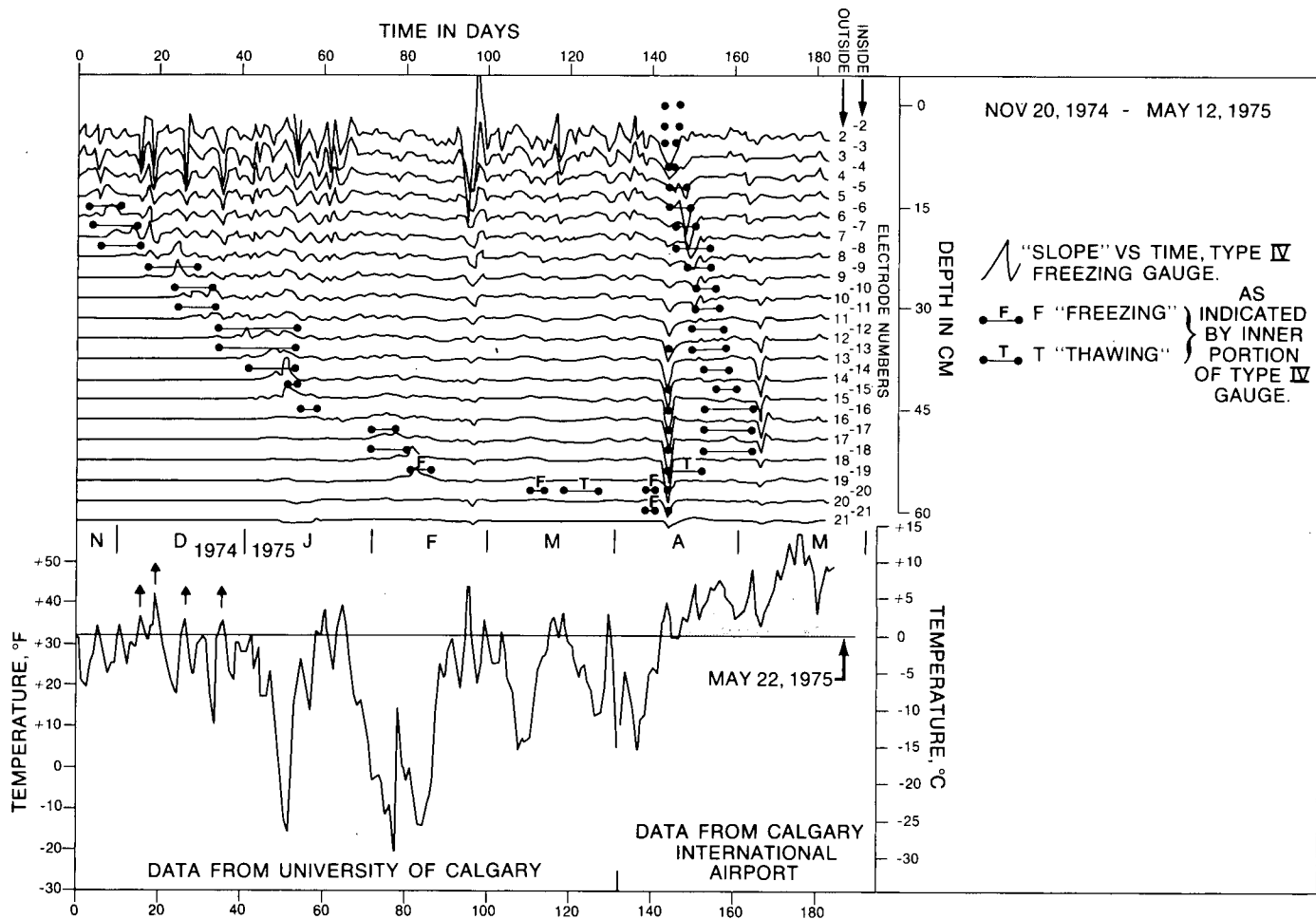


Figure 11. "Slope" of resistance vs. time for individual electrodes of the type IV freezing gauge at the experiment site, 1974-75.

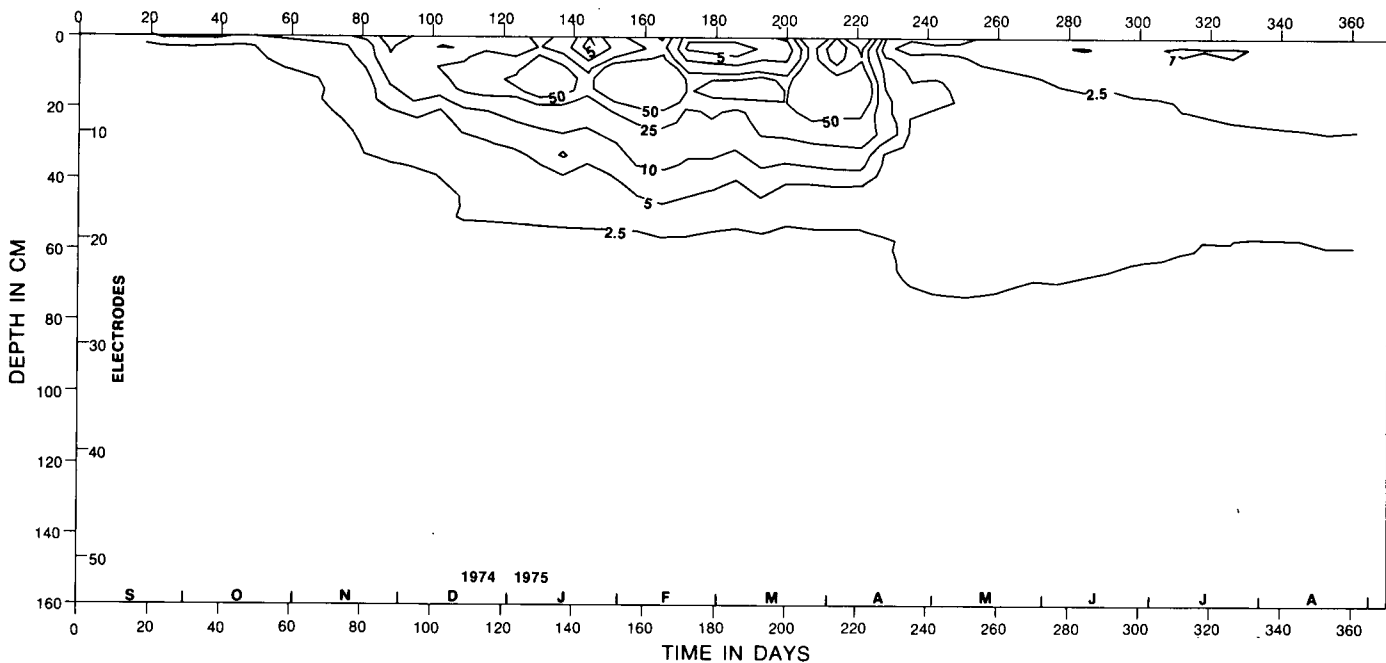


Figure 12. Resistance (in $k\Omega$) as a function of depth and time for the type III frost gauge at the experiment site, 1974-75.

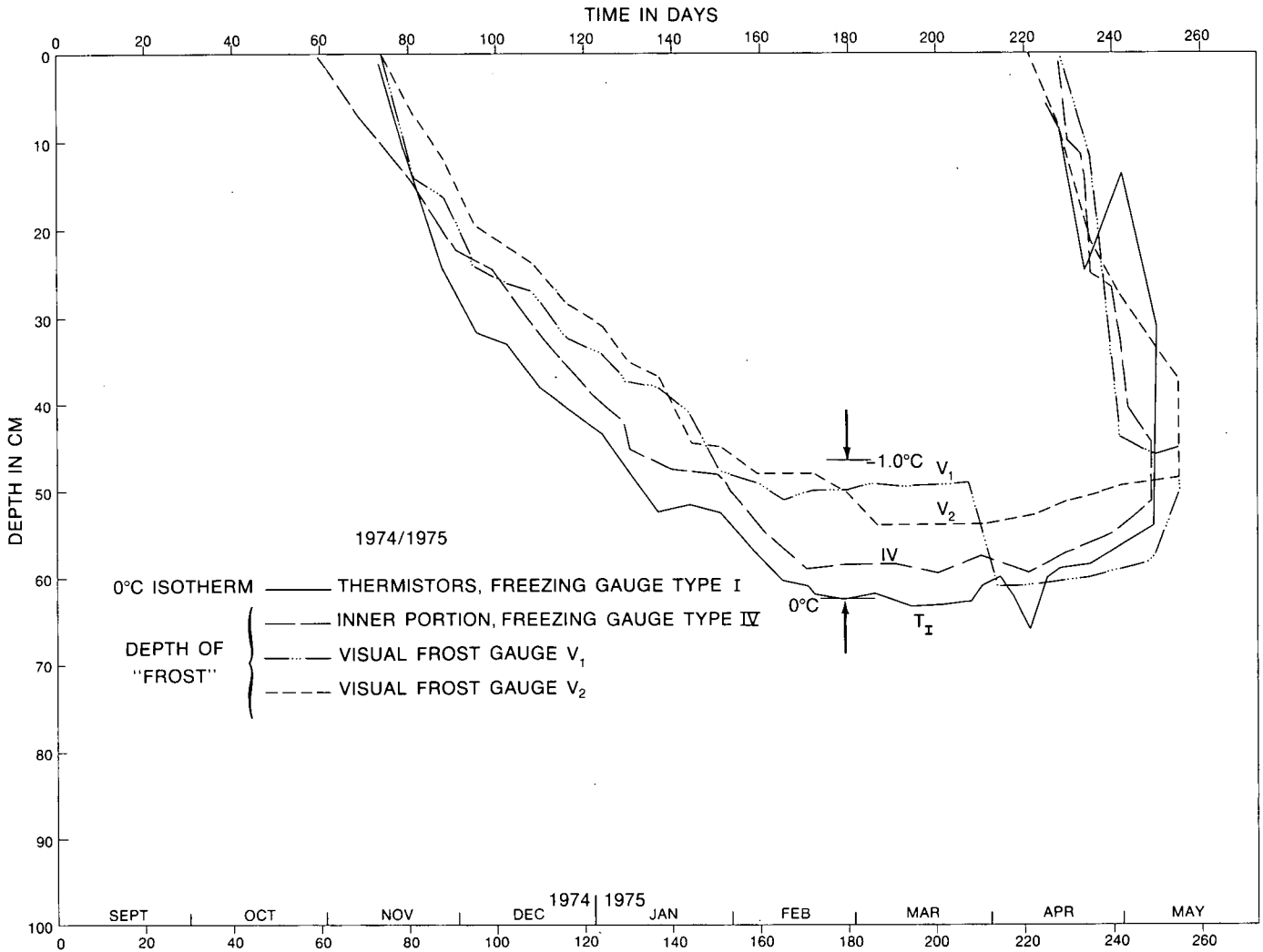


Figure 13. "Possible freezing" period and depth indicated by (a) thermistors in the type I freezing gauge; (b) resistance measured in the type IV frost gauge; and (c) the visual frost gauges V_1 and V_2 at the experiment site, 1974-75.

atures causing them, and their propagation downward can be followed.

So far, only the thermistors in the type I gauge and the inner portion of the type IV gauge have been considered in determining the *possibility* of freezing.

The existence of temperature conditions conducive to freezing can also be determined by the use of the type III frost gauge, for which contoured results are shown in Figure 12, or by visual frost gauges, readings for which are shown in Figure 13. Figure 13 also shows the 0°C isotherm indicated by the thermistors of the type I freezing gauge, and the line enclosing the "area of possible freezing" derived from resistance data from the inner portion of the type IV combination gauge.

COMPARISON OF RESULTS FROM DIFFERENT GAUGE TYPES

Figure 5A shows more gradual penetration of freezing than Figure 5B. A similar but less pronounced difference is noticeable during the thawing period. Also, the ratio between the frozen and nonfrozen resistance for the type I gauge (Fig. 5A) is somewhat higher than that for the type II gauge (Fig. 5B). These obvious differences are, at least in part, the result of the different electrode configurations of the two gauges (Table 1). It is also likely that air convection inside the type II gauge distorts the temperature regime to some extent.

Disregarding the influence of the high-resistance zone around electrode 9 of the type I gauge, a detailed compar-

ison of Figures 7 and 8 shows that the time/depth extent of freezing indicated by the resistance contours for the type IV and type I gauges is similar, even though the two plots are quite different in overall appearance. Resistance values from either gauge can be used to determine the *relative degree* of freezing in time and depth. However, because of differing electrode configurations, resistance values from one gauge type should not be compared with those from another type.

Comparison of Figure 9, which shows bunched contours for the inner portion of the directly buried type IV gauge, with Figure 12, which shows more widely separated contours for a type III gauge installed in an access tube, reveals that the type III gauge suffered from a slow rate of freezing and thawing and that it began to freeze and thaw too soon. This can be attributed to the air circulation in the annular space between the gauge and the access tube, and to the exposure of the top of the black plastic tube above the snow.

Comparison of the resistance data from the inner portion of the type IV gauge (Fig. 9) with the temperature data from the thermistors of the type I gauge (Fig. 13) indicates early freezing inside the type IV gauge, probably as a result of accelerated heat loss via the upper end that protruded above the snow; this was followed by a lag in freezing due probably to the freezing-point depression in the tap water with which the gauge was filled. Comparison of the visual frost gauge results with the thermistor results indicates an even greater lag in freezing (probably owing to the higher concentration of dissolved solids), after an initial close agreement that was probably a fortuitous result of the lag in freezing being balanced by the tendency to freeze too soon because of heat loss via the upper end protruding above the snow.

From the one-degree interval marked at day 179 on Figure 13, the freezing-point depression in the inner portion of the type IV gauge appears to be about 0.25°C , and that in the visual gauges about 0.79°C .

RELIABILITY

Changes in Contact Resistance with Time

Corrosion of electrode materials could affect measured resistance values to a gradually increasing degree. For this reason, only stainless steel or galvanized steel electrodes were used.

Tests were made to determine whether any cumulative changes in contact resistance occurred with time. As

expected, the type III gauge and the inner portion of the type IV gauge, with their stainless-steel electrodes permanently submerged in water, did not show any measurable change in contact resistance when tested with a new filling of tap water.

The results of a test on September 30, 1977, in which the ground around the gauges was thoroughly saturated with water, revealed only small changes in contact resistance for the type I and type IV gauges. It appears that in the five years since its installation the average resistance value measured for saturated conditions by the type I gauge increased by 7 ohms, from 398 to 405 ohms (or slightly over half the difference in resistance represented by a single-unit difference in instrument reading). The resistance measured by the outer portion of the type IV gauge under the same conditions appeared to have increased by about 5 ohms, from 164 to 169 ohms, or slightly less than half the resistance difference represented by a single-unit difference in instrument reading.

Cumulative Changes in Resistance, Type III Gauges

Cumulative changes in resistance occurred inside the type III gauge and also in the inner portion of the type IV gauge, as a result of expulsion of dissolved solids during the

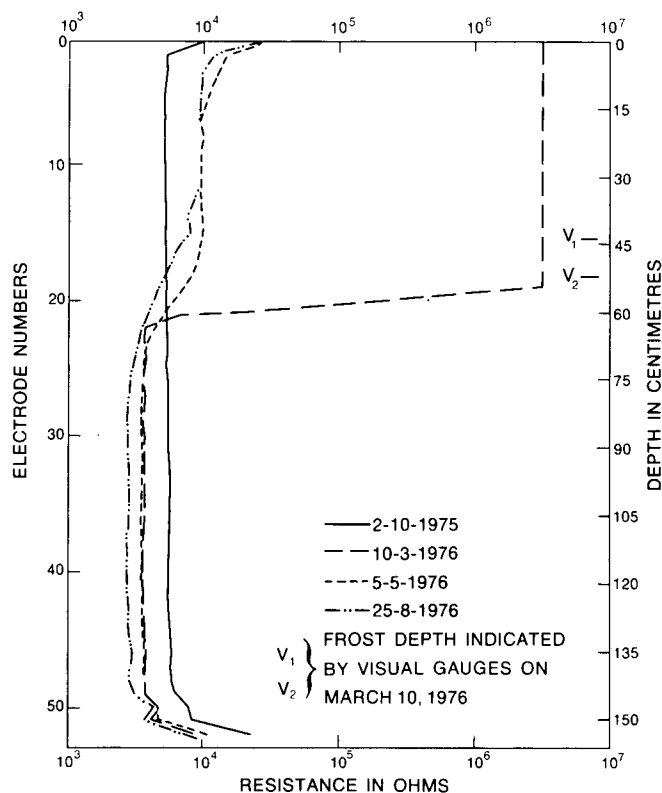


Figure 14. Cumulative changes in resistance in the type III frost gauge at the experiment site, 1975-76.

gradual freezing of the water filling. This produced significantly larger resistance values inside the upper portions of these gauges upon thawing of the filling as compared to the resistance before freezing (Fig. 14). At the same time the resistance in the lower portions of the gauges decreased as a result of increasing dissolved-solids concentration in the water filling. This effect was apparently only partly reversed through diffusion (and possibly some convection) during the frost-free season.

Leakage and Potential Damage from Freezing, Type III Gauge

The type III gauge, installed in an access tube at the experiment site on September 18, 1974, was retrieved on September 30, 1977, and inspected.

The gauge had initially been provided with a filling of water and of styrofoam balls to absorb expansion and prevent buildup of high pressures during freezing of the water. The styrofoam balls were removed in October 1975; from that time onwards the filling consisted of tap water only. Inspection of the gauge after its retrieval indicated that any increase in pressure that might have developed inside the gauge during two winters did not adversely affect the integrity of the gauge.

It was also found that some water leakage had occurred, from the inside tube through the electrode holes to the space between the tube and the rubber wrapping. Leakage to (and contact with) the outside had been prevented by the vulcanized rubber.

CONCLUSIONS

1. In saturated conditions, the type I and type II freezing gauges (and although it was not so tested, probably also the type IV combination gauge) give straightforward, easily interpreted indications of the time/depth extent and relative degree of freezing.
2. In unsaturated conditions, type I and type IV gauges, with their self-contained methods for determining whether or not the possibility (in terms of temperature) exists for freezing to take place, can be used to determine the time/depth extent of actual freezing and they provide an indication of the relative degree of freezing.
3. Freezing gauge data presented in the form of contoured plots are the most useful, but care must be used in the selection of contoured resistance values.

4. Freezing gauge data, presented in the form of resistance vs. time plots for saturated conditions, and in the form of "slope" vs. time plots for unsaturated conditions, enable accurate determination of the time/depth extent of freezing, but the "slope" vs. time method requires more frequent measurements.
5. If data from different gauges are to be compared, the gauges should have identical electrode configurations.
6. For reliable results, electrical-resistance frost and freezing gauges should be buried directly in the ground with carefully tamped, or better, slurried backfill. They should not be installed in access tubes. Above-ground protrusions should be kept to a minimum.
7. There was reasonable agreement between the results from the thermistors, from the inner portion of the type IV combination gauge and from the visual frost gauges. However, the freezing-point depression caused by the dissolved solids required for operation of the visual frost gauges, as well as their protrusion above the snow, excludes them when accurate determination of the time and depth at which freezing can occur is desired. Nevertheless, their low cost and ease of construction and operation make visual frost gauges attractive for many practical applications.
8. Electrical freezing gauges could be most useful in applications dealing with geological materials exhibiting large and variable freezing-point depressions.

REFERENCES

- Anderson, D.M. and Morgenstern, N.R. 1973. Physics, chemistry and mechanics of frozen ground. *Permafrost: The North American Contribution to the Second International Conference*, U.S. National Academy of Sciences, Washington, D.C., 1973, pp. 257-288.
- Colman, E.A. and Hendrix, T.M. 1949. The fiberglass electrical soil-moisture instrument. *Soil Sci.* 67:425-438.
- Garstka, W.V. 1944. Hydrology of small watersheds under winter conditions of snow cover and frozen soil. *Transactions American Geophysical Union*, Part IV, pp. 838-871.
- Harlan, R.L., Banner, J.A. and Freeze, R.A. 1971. Interpretation of electrical-resistance soil moisture data for a freeze-thaw environment. *Can. J. Soil Sci.* 51:249-259.
- Hoekstra, P. and McNeill, D. 1973. Electromagnetic probing of permafrost. *Permafrost: The North American Contribution to the Second International Conference*, U.S. National Academy of Sciences, Washington, D.C., 1973, pp. 517-526.
- Mackay, J. Ross. 1973. A frost tube for the determination of freezing in the active layer above permafrost. *Can. Geotech. J.* 10(3):392-396.

Rickard, W. and Brown, J. 1972. The performance of a frost-tube for the determination of soil freezing and thawing depths. *Soil Sci.* 113(2): 149-154.

Sartz, R.S. 1967. A test of three indirect methods of measuring depth of frost. *Soil Sci.* 104: 273-278.

van Everdingen, R.O. and Banner, J.A. 1975. Groundwater-level and ground-temperature observations, Norman Wells, N.W.T. *In* Hydrology Research Division, Summaries of Progress and Short Research Reports, Inland Waters Directorate, Report Series No. 42, pp. 65-74.